ORIGINAL ARTICLE

WILEY The Prostate

Influence of the neural microenvironment on prostate cancer

Christian Coarfa[1] | Diego Florentin[2] | NagiReddy Putluri[1] | Yi Ding[3] |
Jason Au[4] | Dandan He[5] | Ahmed Ragheb[6] | Anna Frolov[7] |
George Michailidis[7] | MinJae Lee[8] | Dov Kadmon[4] | Brian Miles[9] |
Christopher Smith[4] | Michael Ittmann[10] | David Rowley[1] | Arun Sreekumar[1] |
Chad J. Creighton[7] | Gustavo Ayala[3]

[1] Department of Molecular & Cell Biology, Baylor College of Medicine, Houston, Texas

[2] Department of Internal Medicine, Detroit Medical Center, Wayne State University, Sinai-Grace Hospital, Detroit, Michigan

[3] Department of Pathology and Laboratory Medicine, University of Texas Health Sciences Center Medical School, Houston, Texas

[4] Scott Department of Urology, Baylor College of Medicine, Houston, Texas

[5] Diana Helis Henry Medical Research Foundation, New Orleans, Louisiana

[6] Faculty of Medicine, Department of Urology, Beni Suef University, Beni Suef, Egypt

[7] Dan L. Duncan Cancer Center, Baylor College of Medicine, Houston, Texas

[8] Biostatistics/Epidemiology/Research Design (BERD) Core, Department of Internal Medicine, University of Texas Health Sciences Center Medical School, Houston, Texas

[9] Department of Urology, The Methodist Hospital, Houston, Texas

[10] Department of Pathology & Immunology, Baylor College of Medicine, Houston, Texas

Correspondence
Gustavo E. Ayala, MD, Department of Pathology and Laboratory Medicine, University of Texas Health Sciences Center Medical School, 6431 Fannin Street, Houston 77030, Texas.
Email: gustavo.r.ayala@uth.tmc.edu

Background: Nerves are key factors in prostate cancer (PCa), but the functional role of innervation in prostate cancer is poorly understood. PCa induced neurogenesis and perineural invasion (PNI), are associated with aggressive disease.

Method: We denervated rodent prostates chemically and physically, before orthotopically implanting cancer cells. We also performed a human neoadjuvant clinical trial using botulinum toxin type A (Botox) and saline in the same patient, before prostatectomy.

Result: Bilateral denervation resulted in reduced tumor incidence and size in mice. Botox treatment in humans resulted in increased apoptosis of cancer cells in the Botox treated side. A similar denervation gene array profile was identified in tumors arising in denervated rodent prostates, in spinal cord injury patients and in the Botox treated side of patients. Denervation induced exhibited a signature gene profile, indicating translation and bioenergetic shutdown. Nerves also regulate basic cellular functions of non-neoplastic epithelial cells.

Conclusion: Nerves play a role in the homeostasis of normal epithelial tissues and are involved in prostate cancer tumor survival. This study confirms that interactions between human cancer and nerves are essential to disease progression. This work may make a major impact in general cancer treatment strategies, as nerve/cancer interactions are likely important in other cancers as well. Targeting the neural microenvironment may represent a therapeutic approach for the treatment of human prostate cancer.

KEYWORDS
Botox, cancer, denervation, nerves, neurogenesis, prostate

1 | INTRODUCTION

Nerves are critical regulators in the prostate. They are involved in the embryologic development of the pelvic floor[1,2] as well as the homeostasis of the non diseased prostate.[3-10] Nerve-regulated functions are also important for wound repair and tissue homeostasis.[11-13] Nerves in the prostate peak in young adulthood, and then decrease with age.[14-16]

Nerves and blood vessels co-evolve developmentally and are important components of the tumor microenvironment, along with carcinoma-associated stromal cells, matrix factors, and immune components. Nerves exhibit inductive and trophic functions during development and in adult tissues. Nerve-regulated functions are also important for wound repair and tissue homeostasis. We previously demonstrated that cancer cells induce axonogenesis/neurogenesis[17] and that the nerve-cancer interaction in perineural invasion results in a survival advantage for cancer cells.[18,19] Accordingly, interactions between nerves and cancer cells likely affect the rates and patterns of cancer aggressiveness, although this has not been directly studied in vivo. Addressing the functional significance of nerve-cancer interactions and identifying the mechanisms of these interactions may lead to new therapeutic approaches to target the neural niche in the cancer microenvironment.

Nerves in the host tumor microenvironment have emerged as key modulators of cancer progression.[20,21] Our group has previously demonstrated that prostate cancer (PCa) induces axonogenesis and neurogenesis. This process starts at the level of the preneoplastic high-grade prostatic intraepithelial neoplasia (HGPIN).[17,22] PCa-induced neurogenesis is regulated, at least partly, by semaphorin 4F.[23] Furthermore, nerve-cancer interactions during perineural invasion (PNI) results in a survival advantage for cancer cells.[18,19,24,25] These phenomena have been demonstrated in many other cancer types,[26-29] demonstrating that nerves have a fundamental role in cancer progression. Addressing the functional significance of nerves and identifying the mechanism by which they influence cancer cell growth may lead to therapeutic approaches that target the neural niche in cancer.

This study confirms that interactions between human cancer and nerves are essential to normal epithelial homeostasis and cancer progression. A human proof-of-principle neoadjuvant Botox chemical denervation clinical trial validates that targeting nerves can be used as a treatment strategy for cancer. This work may make a major impact in general cancer treatment strategies. We believe that our findings are seminal, extensive, and describe a previously unknown biological mechanism underlying prostate cancer pathogenesis that is likely to be relevant to other neoplastic disorders.

2 | MATERIALS AND METHODS

2.1 | Cell lines

VCaP cells that had previously been engineered to express luciferase[7,30] were provided by Dr. Michael Ittmann on passage 10. They were tested for mycoplasma. These cells were maintained in 1× DMEM supplemented with 1% FBS and 1 µg/mL puromycin as an antibiotic/antimycotic. VCaP-luc cells can continuously express the luciferase gene.

2.2 | Animal model experiments

2.2.1 | Rats

All animals were used following IACUC protocol AN-4241 in accordance with all BCM animal policies. Owing to the greater ease of surgical manipulation of the neural anatomy of rats and the relative ease of maintenance of rats post-surgery, we chose a nude rat orthotopic VCaP model initially. Sixty adult male NIH-Foxn1rnu nude rats, each weighing 300-350 g, were obtained from Charles River Laboratories. Nude rats were maintained in a B1 barrier at 22.8°C and 60% humidity under a 12-h dark-light cycle. Animals were monitored for behavior, weight, and food and water intake. Botox® (Botulinum Toxin Type A) was obtained from Allergan (Irvine, CA) in vials containing 100 U of lyophilized toxin and stored at −20°C until use. Experimental procedures were conducted under anesthesia with continuous oxygen flow enriched with 1.5-3% isofluorane (3% for induction and 1.5% for maintenance).

NIH-Foxn1rnu nude rats were divided into seven groups of 10 animals.

1. Unilateral Botox chemical denervation prior to VCaP-luc injection.
2. Bilateral chemical denervation via Botox prior to VCaP-luc injection.
3. Control vehicle saline injections prior to VCaP-luc injection (control for previous two groups).
4. Unilateral physical denervation, prior to VCaP-luc injection through major pelvic ganglia [MPG] excision, 1 week prior to orthotopic injection.
5. Bilateral physical denervation (MPG excision).
6. Sham surgery prior to VCaP-luc injection (control for previous two groups).
7. No treatment (VCaP-luc injection only).

2.3 | General Surgical Procedure

For all groups, an identical surgical procedure was followed. The lower abdominal region of each animal was shaved and disinfected (Betadine®). On day 0, a lower transverse abdominal incision was made. The bladder, prostate lobes, and ductus deferens were carefully dissected. The anterior, lateral, and dorsal lobes of the prostate were exposed and separated from the surrounding tissue, followed by the injection of cells and/or physical denervation as described below. Skin was closed using surgical clips. Rats were provided buprenorphine as a postoperative analgesic and monitored daily for signs of infection and morbidity.

2.4 | Physical Denervation

After exposure of the prostate, the ductus deferens was carefully moved off the lateral lobe to access the MPG on the lateral aspect of

the dorsal lobe. The MPG was located and dissected on one (for unilateral denervation) or both sides (for bilateral denervation) by identifying its four main branches and accompanying vessels before it was excised to ensure complete physical denervation on that side and minimize damage to vessels. Homeostasis was carefully maintained during the procedure. For validation, the removed MPGs were fixed in 10% neutral buffered formalin, embedded in paraffin, sectioned, and evaluated histologically to confirm complete excision and hence denervation. As a control, all steps prior to the actual MPG excision were mimicked in the sham surgery group.

2.5 | Chemical denervation

Botox was reconstituted in 0.1 mL of 0.9% saline without preservatives to a concentration of 1 U/μL and used within 2 h of reconstitution. Ten units of Botox per prostate (or volume-matched 0.9% saline vehicle) were slowly injected into one point of the dorsolateral lobe of one (unilateral group) or both sides (bilateral group) using a 30-gauge needle and precise glass syringe with caution to avoid extraprostatic leakage. Care was taken to administer the same volume of 10 μL to each prostate. The same technique was used to inject saline, which is the vehicle for Botox dilution, in the control group.

2.6 | VCaP-luc cells orthotopic inoculation

On Day 8, 2×10^6 VCaP-luc cells at a concentration of 5×10^4 cells/μL were slowly injected into one point of the dorsolateral lobe of one or both sides using a 30-gauge needle, following the same injection technique previously described for chemical denervation. The needle used for injection was exchanged for each rat to avoid the sedimentation of cells in the plastic hub, which can potentially result in inaccurate injection.

2.7 | Autopsy and tissue analysis

We selected histologic image analysis quantitation as our endpoint due to unreliable IVIS imaging results due to size of the animals and depth of the prostate. Postoperatively, the rats were monitored daily. Lower abdominal palpation of the prostate was performed weekly starting 3 weeks after VCaP-luc inoculation to monitor tumor progression. Palpable tumors were observed starting in the 7th week after inoculation. All animals were subsequently sacrificed at 7 weeks. The prostate of each animal was dissected, excised, weighed with and without the seminal vesicles and bladder after separation, and processed for histopathology and RNA extraction as described below.

2.8 | Histologic examination and image analysis

Prostate tumors were sectioned following the largest axis of the tumor in halves. One section was fixed with optimal cutting temperature compound (Tissue-Tek®), deposited in nitrogen liquid, and stored at −20°C, and the matching half was fixed in 10% buffered formalin overnight at room temperature and processed for histopathology and

immunohistochemistry. Sections from both the paraffin embedded and the frozen tissues were stained with hematoxylin and eosin. Slides were fully imaged using the Trestle system. Tumors were mapped on the slides and area of tumor was analyzed using NIH image J measured in pixels.

Representative samples of the liver, lungs, and spinal cord with the entire brain were harvested and processed for histologic analysis. No metastases were identified in any cohort group.

2.8.1 | Nude mice

In a confirmatory experiment, athymic NCr-nu/male homozygous nude mice, 5-6 weeks of age, were purchased from NCI-Frederick. Transgenic mice were not used as they do not survive the side effects related to denervation (neurogenic bladders/recti). Nude mice were maintained under constant environmental conditions (22.8°C, 60% humidity and 12:12 h dark-light cycle). Experimental procedures were conducted under anesthesia with continuous oxygen flow enriched with 1-2% isoflurane. VCaP PCa cells have been previously described. These cells were maintained in DMEM supplemented with 10% FBS and 1 ug/mL puromycin.

Two hundred and twenty five nude mice weighing 28-31 g (at age of 11 weeks) were divided into five groups:

1. Saline + Vcap-luc (control, $n = 45$) as control for groups 2 and 3; (final $n = 32$ mice).
2. Botox + Vcap-luc ($n = 50$); (final $n = 30$ mice).
3. Bilateral Botox + Vcap-luc ($n = 50$); (final $n = 32$ mice).
4. Spinal cord injury + Vcap-luc ($n = 40$); (final $n = 17$ mice).
5. Vcap-luc alone ($n = 40$), as control for group 4. (final $n = 29$ mice).

At age of 11 weeks, mice in groups 1-4 had their initial surgical intervention (saline/Botox injection, castration or spinal cord injury). At age of 13 weeks, all mice prostates were injected with Vcap-luc. Mice in Group 5 only had one intervention, Vcap-luc injection. Botox was reconstituted in saline without preservatives and used within 3 h of reconstitution. Group 2 received 0.45 units (in15 uL saline) of Botox (or volume-matched saline) and Group 3 received 0.45 units (in 20 uL saline) of Botox.

To access the abdominal cavity, a transverse incision was made and the major genitourinary organs identified. Botox were slowly injected into one ventral lobe (group 2) or both ventral lobes (group 3, bilateral Botox injection, 10 uL/lobe), using a 30 gauge needle and precise glass syringe with caution to avoid extra-prostatic leakage during the injection. The same technique was used to inject saline (group 1), which is the vehicle for Botox. Skin and abdominal muscle was closed with surgical staples.

Using the assistance of a surgical microscope, T8-10 laminectomy and spinal cord resection was performed in group 6 as surgically induced spinal cord injury, and thus denervate at the prostate. Immediately after the procedure, paraplegia of both hind legs was confirmed. Rodent food and hydro-gel (in petri dish) was given at cage floor for easy reach, and cages were changed daily to keep the cage clean.

Two weeks after the first surgery, 1 million of VCaP-luc cells in 15 uL PBS (groups 1, 2, 4, and 5) were slowly injected into right ventral lobe (groups 1, 2, 4, and 5) or both ventral lobes (groups 3, 10 uL/per lobe), using a 30 gauge needle, following the same injection technique described above.

Two other additional groups were performed to address hormonal influence:

1. Castration.
2. Castration + Bilateral Botox.

Bilateral orchiectomy was performed on mice in groups 3 and 4 for surgical castration. Using the assistance of a surgical microscope, T8-10 laminectomy and spinal cord resection was performed in group 6 as surgically induced spinal cord injury, and thus denervate at the prostate. Immediately after the procedure, paraplegia of both hindlegs was confirmed. Rodent food and hydro-gel (in petri dish) was given at cage floor for easy reach, and cages were changed daily to keep the cage clean.

2.9 | Imaging and quantification of bioluminescence data

Tumor growth was assessed at 3 and 6 weeks after Vcap-luc injection using the IVIS imaging system (Xenogen, Caliper Life Sciences). Mice were anesthetized with a mixture of 1.5% isoflurane/air using an Inhalation and Anesthesia System (VetEquip, Inc., Pleasant Hill, CA), and imaged 5 min after D-luciferin (Molecular Probes) injection (25 mg/ kg i.p.). A region of interest (ROI) was manually selected over relevant regions of signal intensity. The area of ROI was kept constant within experiments and the intensity was recorded as total photon counts per second per cm^2 within a ROI. A background area with no signal was selected, and subtracted from total photons from the ROI to attain the true signal intensity.

2.10 | Autopsy

Mice were sacrificed at 7 weeks after Vcap-luc injection and prostate, tumor and seminal vesicles were weighed and recorded. Prostates were examined for gross and histopathologic presence of tumor. Differences in mean tumor size and image signal were analyzed by t-test.

2.11 | Laser-capture Microdissection of Human Prostate Tumors

Tissues were laser captured from three sources:

1. Rat tissues.
2. Human tissues from two of the patients treated with Botox (saline side and Botox side separately).
3. Human tissues from a patient that developed PCa after spinal cord injury. Tissues from a patient with intact nerve function and matched Gleason and stage were used as control.

In all groups, we laser captured the normal epithelium, the cancer and the stroma. Frozen sections (8 μm) were prepared with a cryostat from tissue cores of normal and cancerous areas of fresh, unfixed prostatectomy specimens. Frozen sections were placed on non-charged glass slides and stored at −80°C before use. Slides were stained and dehydrated according to the manufacturer's protocol. Laser-capture microdissection was performed using a Pixcell II laser-capture microdissection microscope (Molecular Devices). Approximately 4,000-8,000 laser pulses of PCa and normal prostate tissues were captured on 2-3 caps (1,500-1,500 spots).

2.12 | Total RNA extraction-amplification and cDNA microarray analysis

Total RNA was extracted from frozen section slides by laser-capture microdissection of epithelium, stroma, and tumor compartments of rat and human tissues using a PicoPure RNA Isolation Kit (Molecular Devices). RNA was then amplified using a RiboAmp TM RNA Amplification Kit (Two rounds). The cDNA reverse transcription and fluorescent labeling reactions were performed using the Invitrogen SuperScript Plus Direct cDNA Labeling System with Alexa Fluor S ′-Aminohexylacrylamido-dUTP (Invitrogen). The cDNA microarray was performed as previously described.[18]

2.13 | Neoadjuvant botox phase 1 clinical trial

This is a pilot study examining biological endpoints in men with localized PCa who are scheduled to have radical prostatectomies. Four patients with bilateral localized PCa were recruited to a Phase I/II clinical trial: Neoadjuvant Botox injection prior to radical prostatectomy (NCT01520441), (IRB: H-25362). The trial was designed as a proof of principle that nerves affect the biology of PCa in humans. The inclusion criteria were as follows: male and at least 50 years of age; biopsy-proven, clinically localized PCa; low risk for recurrence defined as a Kattan nomogram score of less than 115, serum PSA <10 ng/mL, individual Gleason grade of 7 or lower, or clinical stage T2b or below; must have agreed to radical prostatectomy and signed an informed consent; and the patient must be able to complete the study protocol in the opinion of the investigator.

Patients serve as their own controls by receiving Botox injections into the right peripheral and transition zones and sham saline injections into the left peripheral and transition zones. Patients were examined, and urines were tested for infection. Patients received a single dose of broad-spectrum antibiotics the morning of the procedure. Anesthesia was delivered according to clinical practice via a long 22-gauge needle. Patients were injected (ultrasound guided transrectal) with 100 U of Botox in 2 mL of preservative-free saline for transition zone and peripheral zone injections (right prostate lobe). Volume matched preservative-free saline injections were injected into patient's left lobe. Because of the theoretical possibility of the diffusion of Botox into seminal fluid and no evidence to the contrary, those patients who engage in sexual intercourse were required to use condoms for 48 h after the injection.

Four weeks later, a radical prostatectomy was performed following standard clinical practices. Tissues were processed using standardized methodology and frozen tissues obtained from the right and left peripheral and transition zones. The residual tissues were processed in formalin and embedded in paraffin to study biological endpoints.

2.14 | Human tissue studies

The TUNEL assay for apoptosis was performed using the ApopTag Peroxidase InSitu Apoptosis Kit (cat S7100, Millipore). Immunohistochemistry was performed using standardized procedures with the following antibodies: PGP9.5 (Protein Gene Product 9.5) (incubation of primary antibody, AB1, clone 10A1, cat #Ms-1760 NeoMarkers/Thermo Scientific) at 1:30 overnight at 4°C and then 3 h at room temperature); and Ki-67 (incubation of primary antibody (Ki-67 rbMab, cat #RM-9106) at 1:400 for 30 min at room temperature).

2.15 | Imaging and image analysis:

Hot spot areas of expression of biomarkers within the PCa and non neoplastic tissues were imaged using the Nuance image deconvolution system (Four 200× images per area). The InForm image segmentation system was used to separate non neoplastic and neoplastic PCa tissues from the stroma tissues. Signal was analyzed only in the epithelial component in the case of Ki-67 and TUNEL, while the stromal compartment analyzed for PGP 9.5. Nerve density was defined as PGP 9.5 positive structures.

3 | RESULTS

3.1 | Denervation effects on non-neoplastic prostate epithelium

We assessed the effects of denervation on the homeostasis of non-neoplastic prostate epithelium, by rat major pelvic ganglion [MPG] excision or Botox injection (n = 60). Histopathologically, non-neoplastic rat prostate tissue exhibited atrophic histology (Figure 1A-D). This is in agreement with previous studies that show atrophy, changes in protein secretion, and ultrastructural changes within denervated normal epithelium.[2,3,5,7,31–35] Gene expression analysis of laser-captured epithelium or stroma revealed that both chemical and physical denervation produced similar expression profiles that self-clustered in each compartment (Figure 1E). These data confirm that chemical denervation (Botox) produced the same effect on gene expression as physical denervation (MPG). Figure S3A shows the overall concordance between the MPG-induced expression patterns and the Botox-induced expression patterns. An unbiased and global expression analysis for both epithelial and stromal compartments in Botox versus MPG, revealed a significant correlation between the two data sets (Pearson's analysis, rho = 0.55 for epithelial and rho = 0.43 for stromal genes).

A total of 1,231 unique genes were differentially expressed in normal rat prostate epithelium with chemical or physical denervation at a high significance threshold (2237 gene probes, ANOVA $P < 0.01$, SD > 0.2, true positive rate, ~83%). Downregulated genes in denervated prostate were most associated with differentiated functions (Supplemental Data File 1).

To better assess the effects of denervation on tissue homeostasis in general, we also evaluated histologic changes and gene expression patterns in normal rat prostate epithelium in denervated and control conditions. Gene expression profiles in normal rat non-neoplastic epithelium revealed a total of 1,231 unique genes that were differentially expressed at a high significance threshold (2,237 gene probes, ANOVA $P < 0.01$, SD > 0.2, true positive rate, ~83%). Genes that were downregulated as a result of denervation were associated with differentiated functions (Supplemental Data File 2). These included translation and translation initiation factor activity (signal transducer and activator of transcription 3, eukaryotic translation elongation factor 1 gamma*, eukaryotic translation initiation factor 3, subunit J, F, and 9), ribosomes and structural constituents of ribosomes (ribosomal protein L22*, L5, L6, S17, and S6, mitochondrial ribosomal protein S14), and metabolic pathways (ST8 alpha-N-acetyl-neuraminide alpha-2,8-sialyltransferase) (genes denoted by an asterisk were validated by subsequent qRT-PCR using material from a second laser-capture microdissection). Other downregulated genes included proteasome (prosome, macropain) subunit, alpha type 5, protein tyrosine phosphatase domain-containing 1, tyrosine kinase with immunoglobulin-like, and EGF-like domains*, heat shock protein 1-like, cAMP responsive element binding protein 1, forkhead box K2, and RING1 and YY1 binding protein*. Upregulated genes in denervated epithelium were consistent with an acute tissue repair response. Serum response factor, endothelin*, and endothelin receptors types A and B were among the most strongly upregulated genes. Insulin I* and II*, insulin-like growth factor 1, and insulin-like growth factor binding protein 4 were also significantly upregulated. Numerous growth factors were also upregulated including c-fos induced growth factor, connective tissue growth factor, and epidermal growth factor receptor. Fas ligand (tumor necrosis factor superfamily, member 6) and tumor necrosis factor receptor superfamily, member 1b were also upregulated. Additional upregulated genes included those associated with epithelial-to-mesenchymal transition events (collagen, type XVI, alpha 1; type XIV, alpha 1), growth factor expression, and stem cell properties (noggin, secreted frizzled-related protein 4, wingless-related MMTV integration site 11, and dickkopf homolog 4).

Bioprocess mapping of the downregulated gene expression signature mapped to multiple mitochondrial pathways, suggesting an attenuation of cellular bioenergetic metabolism. This finding was further substantiated using targeted metabolic analyses of metabolites belonging to the glycolysis pathway, the pentose phosphate pathway, and the citric acid cycle (TCA). Importantly, levels of TCA metabolites, namely succinate, malate, and fumarate, were significantly (FDR corrected P-value <0.10) down regulated in Botox-treated tissues compared to controls. On the other hand, levels of glucose/fructose and ribose were significantly elevated upon Botox treatment
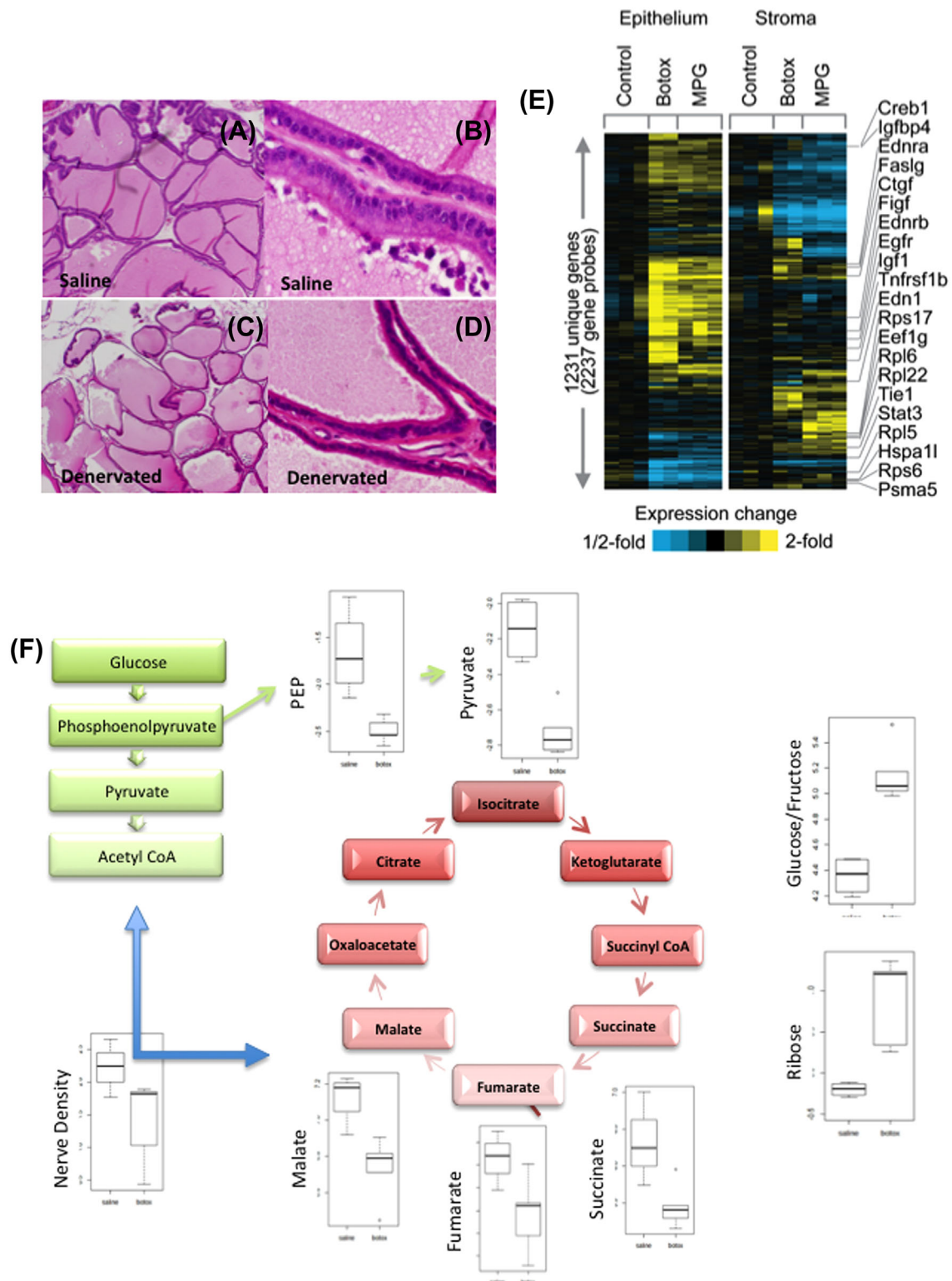
FIGURE 1 Effects of denervation on histopathology of normal rat prostate and human prostate tumors. (A-D) Morphology of non-neoplastic rat prostate epithelium following MPG excision and Botox treatment. Panels A and B (hematoxylin and eosin [H&E], 200× and 600×, respectively) show the epithelium of the non-neoplastic, neurally intact rat prostate. Panels C and D (H&E, 200× and 600×, respectively) indicate the generalized atrophy resulting from physical denervation and Botox treatment. (E) Chemical and physical denervation result in similar gene expression profiles. Cluster expression heat map of the top differentially expressed genes (ANOVA $P < 0.01$, SD > 0.2) in response to Botox or MPG treatment for both epithelial and stromal rat tissues. Rows, genes; columns, profiled samples. Within epithelial and stromal groups, genes are centered on the corresponding control. (F) Targeted metabolomic analysis of Botox-treated tissues show significantly (FDR-adjusted P-value <0.10) reduced levels of metabolites associated with the TCA cycle and elevated levels of glucose/fructose and ribose.

(FDR corrected *P*-value <0.10) (Figure 1F). These findings suggest a shut down in glucose utilization and a potential dependence on gluconeogenesis upon Botox treatment.

3.2 | Prostate denervation results in reduced tumor incidence and size in rodents

To address the *functional significance of neural input to primary PCa*, we denervated prostates in experimental rat and mouse orthotopic VCaP models. Quantitative image analysis of histologic sections demonstrated that bilateral denervation methods resulted in a significant reduction in tumor size (*P* = 0.0196) (Figures 2A and 2B). Additional experiments were performed using a VCaP-luc orthotopic model in nu/nu mice. Botox or saline (vehicle control) were injected uni and bilaterally. Chemical denervation was used to exclude vascular influence. Spinal cord injury (physical denervation) was compared to naïve VCaP-luc injection. Unilateral Botox injection reduced luciferase luminosity detection at 6 weeks (*P* = 0.0005). Bilateral Botox injection reduced luciferase detection both at 33 weeks (*P* = 0.01) (Figure 2D) and 6 weeks (*P* = 0.0007) (Figure 2E), and decreased overall prostate weight (*P* = 0.001) (Figure 2F). Spinal cord injury decreased tumor incidence as measured by gross (*P* < 0.001) and histologic examination (*P* = 0.0004), luciferase detection at 3 weeks (*P* = 0.0002) (Figures 2A, 2H, and 2I), and prostate weight (*P* < 0.0001) (Figure 2F).

Mice were subjected to bilateral orchiectomy alone or with bilateral botox denervation or spinal cord injury. We did not identify significant differences between bilateral botox denervation and spinal cord injury and castration (Figure 2G). As to combined therapies, we did identify significant difference between bilateral botox denervation plus castration versus bilateral botox denervation alone, but not with spinal cord injury. This suggests that there is an opportunity for combined therapies or the improvement of combined therapies to address both the hormonal and the neural axis.

3.3 | Denervation with Botulinum toxin results in increased apoptosis in human PCa

As an initial translational and proof-of-concept study, we evaluated tissues from four patients enrolled in a Phase I clinical trial to assess the effects of Botox injections on biological endpoints (NCT01520441). Patients with bilateral Gleason = <7 tumors received unilateral Botox injections (100 U in a 2.0-mL volume) and vehicle control injection into the contralateral lobe (Figure 3A). Examination of tissue removed at the time of prostatectomy revealed marked morphologic changes on the Botox-injected side, with extensive cancer atrophic and degenerative features, reduced cytoplasm, and pyknotic nuclei (Figures 3H, 3I, and 3L), as compared to features in the saline-injected cancer tissues (Figures 3H and 3I).

A significant increase in apoptosis was observed in both non-neoplastic epithelium (*P* ≤ 0.0001) (Figure 3B) and PCa tissue (*P* = 0.0020) (Figure 3C) following Botox treatment. The findings in the non neoplastic tissues were expected based on our previous findings. Apoptotic cancer cells were also identified in regions of perineural invasion (Figure 3K). No significant changes were observed in the proliferation, as assessed by Ki67 staining. Nerve density was lower in the Botox-injected compared to the control prostate lobes in both the normal epithelium (*P* ≤ 0.0001) (Figure 3D) and in tumor tissue (*P* = 0.0293) (Figure 3D). Microvessel density was slightly decreased in normal tissues (*P* = 0.0015) (Figure 3F), but was increased within tumor tissue (*P* ≤ 0.0001) (Figure 3G).

We did not find a small cell phenotype, or an increase in neuroendocrine markers in our transcriptomic analysis of Botox treated tissues. However, due to the short period of time between Botox injection and the prostatectomy, we do not believe that this data is definitive.

3.4 | Transcriptomic changes in denervated PCa, across species

We evaluated the transcriptomic profiles of laser-captured human cancer cells from denervated rat prostates as compared to intact prostates in order to examine the impact on cellular function. The top Gene Ontology (GO) categories for the downregulated genes included translational elongation, ribosome, structural constituent of ribosome, translation, cytosolic small, and large ribosomal subunit, RNA binding, ribonucleoprotein complex, and protein binding. More importantly, pathways that regulate the cellular energy metabolism were downregulated (mitochondrial pathways, mitochondrial ATP synthesis coupled proton transport, mitochondrial proton-transporting ATP synthase complex, glycolysis, and electron transport chain) (Figure 2C).

The gene expression profile of laser-captured cancer tissue obtained from a PCa patient with a spinal cord injury was examined in an effort to see if the same effect in the rat model was the same in humans. The gene expression pattern in this material was similar to that from cancer cells in denervated rat prostates and in human PCa tissue treated with Botox (Figure 2C). Similar genes were downregulated, whereas differences were observed in upregulated genes between the denervated rat prostate tumor model and the PCa patient with spinal cord injuries. This may reflect the acute nature of the experimental rat denervation model as compared to the chronic denervation in spinal cord injury patients. Finally, transcriptomic analysis of Botox-treated tumors revealed a significantly similar denervation signature profile as identified in the denervated rat orthotopic human tumors (rho = 0.45) or in the human prostate from the spinal cord injury patient (rho = 0.26) (Figure 2C and Figure S3). These data show that a similar gene expression signature can be recognized in mice and humans upon denervation through both chemical and physical methods, suggesting that the effect of nerves on epithelium and cancer tissue is a fundamental biological phenomenon.

4 | DISCUSSION

Previous studies have identified that adrenergic receptors are vital to the development of prostate cancer[20] and of metastatic potential in
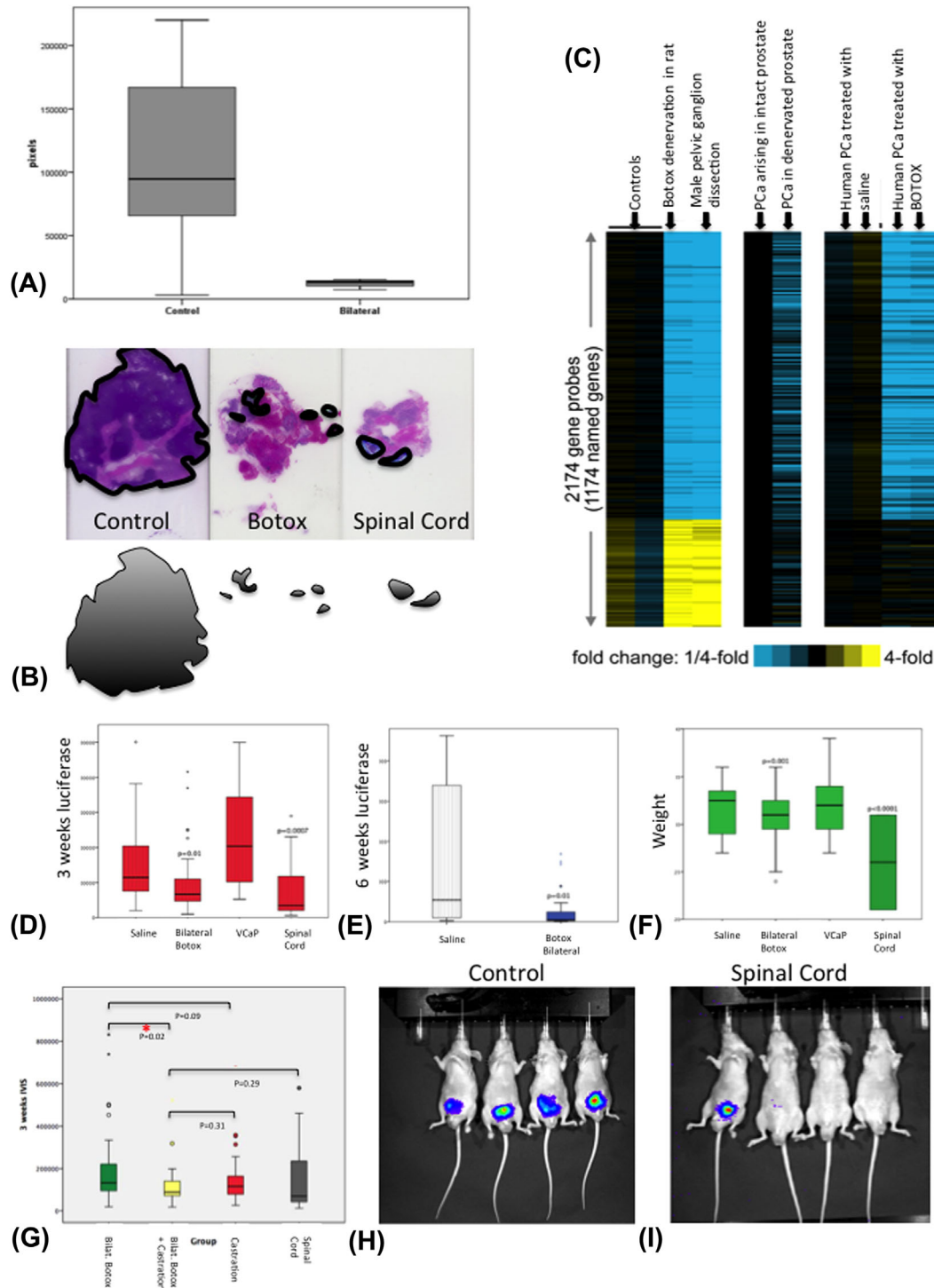
FIGURE 2 (A and B) Tumors evolving in prostates with bilateral denervation with botox and MPG excision are significantly lower than controls (C) Evolving expression profiles of human prostate carcinoma cells growing in denervated rat prostates and in human patients. In the left panel, expression heat maps for genes regulated by both major pelvic ganglion (MPG) dissection and Botox (twofold each) in rats inoculated with VCaP human PCa cells are shown. For these same genes, the corresponding differential patterns are shown for laser-captured carcinoma cells from the prostate of a spinal cord injury patient and the prostate of a patient with intact innervation (middle panel). In the right panel, gene expression profiles in a human PCa patient treated with saline or Botox. MPG/Botox profiles are centered on the corresponding control, whereas denervated versus intact prostate profiles are centered on the normal intact group. Yellow, high expression relative to reference; Blue, low expression. Results of physical and chemical denervation in mouse experiments: (D) Mouse VCaP-luc IVIS luciferase luminosity detection at 3 weeks in the bilateral Botox denervation versus saline and spinal cord injury versus VCaP-only control groups. (E) Luminosity detection at 6 weeks in the bilateral Botox denervation versus saline groups. (F) Overall prostate weight in the bilateral Botox denervation versus saline and spinal cord injury versus VCaP-only control groups. (G) Castration improves the reduction of tumor size over bilateral botox (bilatera), but not over spinal cord injury.
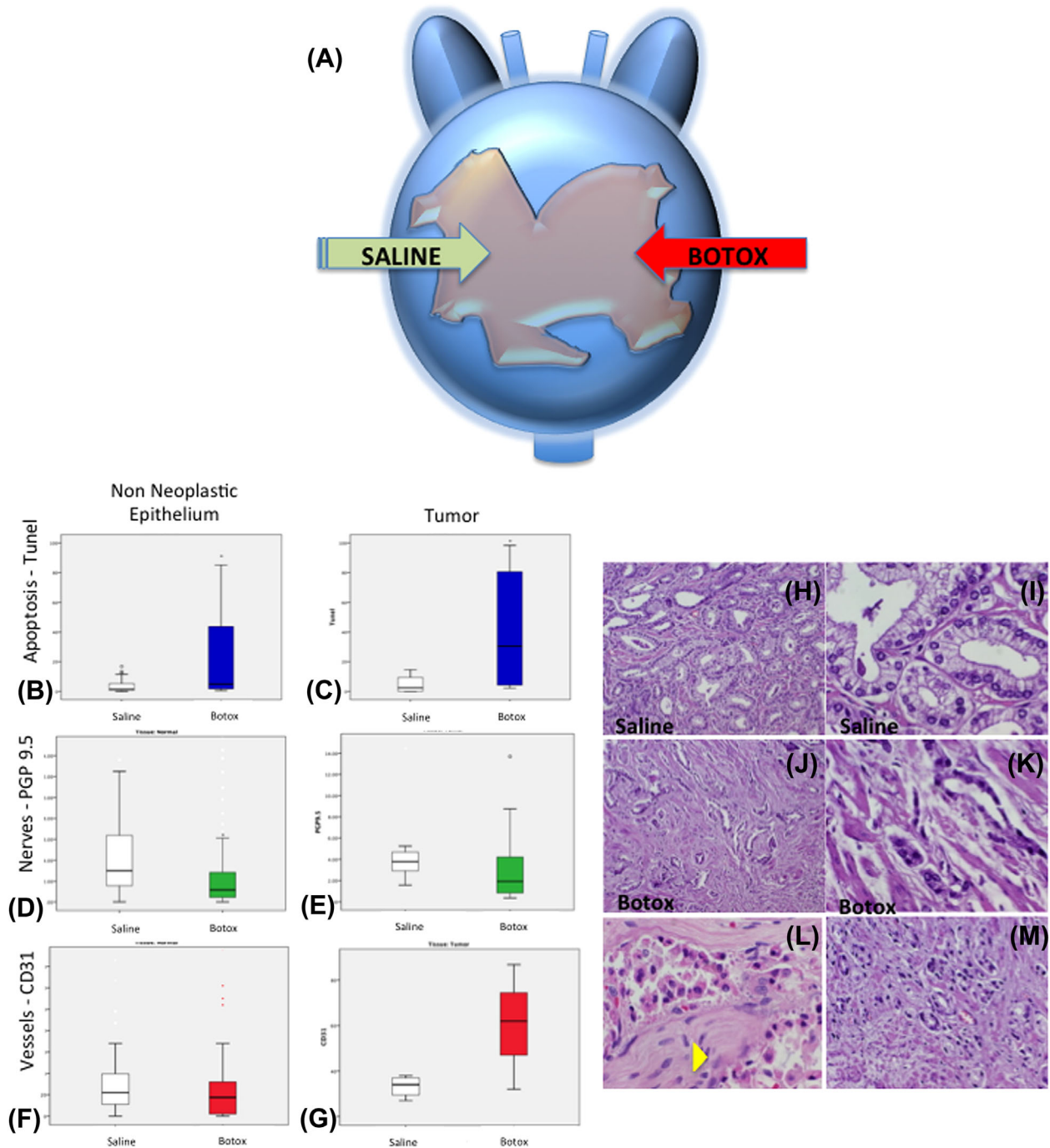
FIGURE 3 (A) Design of the neoadjuvant human proof of principle clinical trial. Botox injected on the right side of the prostate and saline in the contralateral side. (B) Increased apoptotic ratio (TUNEL) in non-neoplastic epithelium treated with Botox versus saline. (C) Similar increased in apoptotic ratio in PCa tissues treated with Botox versus saline. (D-E) Nerve density was decreased in non-neoplastic epithelial prostate tissues and cancer. (F-G) Microvessel density in non-neoplastic tissues and cancer. (H-L) Morphologic changes induced by Botox treatment in human prostate tumors. In the example shown, a patient with bilateral Gleason stage 3 PCa was injected with Botox in the right prostate lobe, and saline in the left prostate lobe as an internal control. Panels J (H&E, 200×) and K (H&E, 600×) show the effects of Botox injection on the PCa tissues, including carcinoma cell involution with reduced cytoplasm and pyknotic nuclei, as compared to intact histology for Gleason 3 PCa observed in the contralateral lobe injected with saline (Panels H [H&E, 200×] and I [H&E, 600×]). (K) Nerve (Yellow arrowhead) surrounded by dead cancer cells with nuclear pyknosis and cytoplasmic disruption (H&E, 600×). (L) PCa cells treated with Botox showing degenerative features associated with cancer death (H&E, 400×).

breast cancer[36] and that beta-2 adrenergic receptors and Her2 are part of a positive feedback loop in human breast cancer cells.[37] In vivo experiments in an orthotopic prostate cancer PC3 model demonstrated that metastasis can be reduced through beta blocker therapy.[38] Furthermore, clinical trials indicate that patients undergoing adrenergic receptor blockade for benign prostate hyperplasia have a lower incidence of prostate cancer than the general population.[39] However, most of this work focuses on molecules, that can be produced by cancer cells and/or excreted by nerves. In contrast, our previous work has specifically explored the relationship between that prostate cancer cells and nerves. PCa induces axonogenesis and neurogenesis and that this process is associated with a more aggressive disease phenotype.[17] Moreover, perineural invasion provides a survival advantage to cancer cells.[18,19]

The studies presented in this article demonstrate the functional significance of nerves in PCa and identify that nerve-cancer cell interactions as critical for epithelial homeostasis and PCa cell energetic metabolism. These studies suggest that nerves exert trophic effects on prostate cancer cells through the regulation of basic cellular processes such as gene expression, protein translation, and metabolism. Together, the experimental tumor study, preliminary Phase I Clinical trial study, and gene expression analysis of prostate tumors from patients with spinal cord injuries suggest that the nerve-cancer cell interaction is a key and critical element in prostate cancer cell survival and tumorigenicity. Tumors in denervated prostates are significantly smaller. Chemical denervation results in nerve atrophy, cancer cell apoptosis in human cancer, while the vascular component remains stable. Hence, it follows that the evolution of cancer initiation and tumor development likely is fundamentally influenced by intact innervation and that the nerves provide a pro-tumorigenic environment.

These studies suggest that the specific mechanisms and pathways that regulate and mediate interactions between nerves and cancer cells are candidate targets for unique therapeutic approaches. Nerve inhibition results in changes in the energetic metabolism of cancer cells, as well as increased apoptosis. It is likely that the increased apoptotic effect found with general denervation, is due to downstream effects of these metabolic changes, not sustainable in the long term. Nerves are critical to the sustenance of basic cellular functions in PCa. This process may have similarities to the general Wharburg effect, where cells and tissues attempt to become more energy efficient as a consequence of a switch to a pro-survival metabolism that results from many conditions. When denervated, our data suggests that the prostate gland change their efficiencies and that this change is similar to the pro-survival changes that evolve in carcinogenesis in the intact gland. These conditions represent a major change in tissue homeostasis and it would appear this general switch in metabolism and cell biology results in similar gene expression profiles.

Nerves provide a fundamental trophic effect not only on PCa cells, but also on non neoplastic prostate epithelium, both at the levels of translation and bioenergetics. Nerves are necessary in wounding re-epithelialization, which is impaired following denervation.[11,12] Furthermore, during development, the formation of the mouse pelvic floor is regulated by the androgen-dependent survival of a neuronal nucleus in the lower spinal cord.[1] Therefore, the effects of nerves on epithelial cells are not exclusive to cancer, as demonstrated by our data. We believe that this process is exploited by cancer.

In conclusion, it is likely that neural axis is a major pathway of homeostasis in prostate cells and tissue. It follows that this is hence, a major mechanism that also regulates cancer cell survival, translation, metabolism, and progression. The neural axis is critical for epithelial and cancer regulation. We foresee potential neurotoxin applications in several therapeutic windows: as a preventive strategy for preneoplastic lesions; local therapy for low risk tumors; adjuvant to surgery (in the biopsy cavity), to reduce recurrence rates; in combination with chemo or targeted therapies; or neoadjuvant to radiation therapy or surgery in large tumors with high probability of recurrence. Combination therapies with anti-androgen therapy need to be explored, as nerves and androgens such as testosterone have been shown to interact.[40] Furthermore, it is likely that nerve-epithelial interactions occur in a wide variety of cancers.[26,28] Hence, the use of neurotoxins should be evaluated in other carcinoma models.

ACKNOWLEDGMENTS

CONFLICT OF INTEREST

The Authors have no conflicts to report that they believe could be construed as resulting in an actual, potential, or perceived conflict of interest with regard to the manuscript submitted for review.

AUTHORS' CONTRIBUTIONS

DF, AR, and JA contributed to the design of the study, the animal experiments, laboratory examinations, collection and analysis of data, discussion, and writing of the manuscript. DH contributed the pathological and immunohistochemical analysis of mice and rat tissues, discussion, and writing of the manuscript. CJC, AF, GM, and YZ contributed the bioinformatics analysis, discussion, and writing of the manuscript. CC, NP, and AS contributed in the metabolomics study design and performance, discussion, and writing of the manuscript. OD contributed the microarray experiment of mice and humans, discussion, and writing of the manuscript. MM contributed in the design and discussion and writing of the manuscript. YD contributed the microarray experiment of mice,

and humans, the in vitro experiments, discussion, and writing of the manuscript. CS, DK, and BM contributed in the design and execution of the human clinical trial, discussion and writing of the manuscript. MI contributed the coordination of pathological evaluation of humans, discussion, and writing of the manuscript. DR contributed the design of the study, the writing of the manuscript, obtaining funding, and discussion, and writing of the manuscript. GA contributed the idea and hypothesis, conception and design of the study, development of the experimental mouse models, collection, analysis and interpretation of data, drafting of the manuscript, obtaining funding, and study supervision and coordination.

ORCID

Gustavo Ayala iD http://orcid.org/0000-0002-5288-0244

REFERENCES

1. Bitoh Y, Shimotake T, Sasaki Y, Iwai N. Development of the pelvic floor muscles of murine embryos with anorectal malformations. *J Pediatr Surg*. 2002;37:224–227.
2. Wang JM, McKenna KE, McVary KT, Lee C. Requirement of innervation for maintenance of structural and functional integrity in the rat prostate. *Biol Reprod*. 1991;44:1171–1176.
3. Kato T, Watanabe H, Shima M, Kaiho H. Studies on the innervation of prostate. 2. Histological changes of the dog prostate after transsection of its innervating nerves. *Nippon Hinyokika Gakkai Zasshi*. 1971;62: 704–707.
4. Watanabe H. Tissue respiration of the partially denervated dog prostate. *Tohoku J Exp Med*. 1968;95:193–199.
5. Watanabe H, Shima M, Kojima M, Ohe H. Dynamic study of nervous control on prostatic contraction and fluid excretion in the dog. *J Urol*. 1988;140:1567–1570.
6. Watanabe H, Kato H, Kato T, Morita M, Takahashi H. Studies on the innervation of the prostate. I. Tissue respiration of the dog prostate after the cutting off of the various innervating nerves. *Nippon Hinyokika Gakkai Zasshi*. 1967;58:381–385.
7. Doggweiler R, Zermann DH, Ishigooka M, Schmidt RA. Botox-induced prostatic involution. *Prostate*. 1998;37:44–50.
8. Lujan Galan M, Paez Borda A, Llanes Gonzalez L, Berenguer Sanchez A. Effect of sacral roots block in the prostatic structure of the rat. *Actas Urol Esp*. 2000;24:516–521.
9. Lujan Galan M, Paez Borda A, Hernandez Lopez C, Baldonedo Rodriguez E, Berenguer Sanchez A. [Ultrastructural morphometric study of the prostate of the rat after microsurgical denervation]. *Actas Urol Esp*. 1998;22:388–394.
10. Baptista CA, Gershon TR, Macagno ER. Peripheral organs control central neurogenesis in the leech. *Nature*. 1990;346:855–858.
11. Barker AR, Rosson GD, Dellon AL. Wound healing in denervated tissue. *Ann Plast Surg*. 2006;57:339–342.
12. Stelnicki EJ, Doolabh V, Lee S, et al. Nerve dependency in scarless fetal wound healing. *Plast Reconstr Surg*. 2000;105:140–147.
13. Smith AR, Wolpert L. Nerves and angiogenesis in amphibian limb regeneration. *Nature*. 1975;257:224–225.
14. Baumgarten HG, Falck B, Holstein AF, Owman C, Owman T. Adrenergic innervation of the human testis, epididymis, ductus deferens and prostate: a fluorescence microscopic and fluorimetric study. *Z Zellforsch Mikrosk Anat*. 1968;90:81–95.

15. Gosling JA, Thompson SA. A neurohistochemical and histological study of peripheral autonomic neurons of the human bladder neck and prostate. *Urol Int*. 1977;32:269–276.
16. Jungblut T, Aumuller G, Malek B, Melchior H. Age-dependency and regional distribution of enkephalinergic nerves in human prostate. *Urol Int*. 1989;44:352–356.
17. Ayala GE, Dai H, Powell M, et al. Cancer-related axonogenesis and neurogenesis in prostate cancer. *Clin Cancer Res*. 2008;14: 7593–7603.
18. Ayala GE, Wheeler TM, Shine HD, et al. In vitro dorsal root ganglia and human prostate cell line interaction: redefining perineural invasion in prostate cancer. *Prostate*. 2001;49:213–223.
19. Ayala GE, Dai H, Tahir SA, et al. Stromal antiapoptotic paracrine loop in perineural invasion of prostatic carcinoma. *Cancer Res*. 2006;66: 5159–5164.
20. Magnon C, Hall SJ, Lin J, et al. Autonomic nerve development contributes to prostate cancer progression. *Science*. 2013;341: 1236361.
21. Zhao CM, Hayakawa Y, Kodama Y, et al. Denervation suppresses gastric tumorigenesis. *Sci Transl Med*. 2014;6:250ra115.
22. Olar A, He D, Florentin D, Ding Y, Ayala G. Biologic correlates and significance of axonogenesis in prostate cancer. *Hum Pathol*. 2014;45:1358–1364.
23. Ding Y, He D, Florentin D, et al. Semaphorin 4F as a critical regulator of neuroepithelial interactions and a biomarker of aggressive prostate cancer. *Clin Cancer Res*. 2013;19:6101–6111.
24. Ayala GE, Dai H, Li R, et al. Bystin in perineural invasion of prostate cancer. *Prostate*. 2006;66:266–272.
25. Ayala GE, Dai H, Ittmann M, et al. Growth and survival mechanisms associated with perineural invasion in prostate cancer. *Cancer Res*. 2004;64:6082–6090.
26. Albo D, Akay CL, Marshall CL, et al. Neurogenesis in colorectal cancer is a marker of aggressive tumor behavior and poor outcomes. *Cancer*. 2011;117:4834–4845.
27. Liebig C, Ayala G, Wilks JA, Berger DH, Albo D. Perineural invasion in cancer: a review of the literature. *Cancer*. 2009;115: 3379–3391.
28. Dai H, Li R, Wheeler T, et al. Enhanced survival in perineural invasion of pancreatic cancer: an in vitro approach. *Hum Pathol*. 2007;38: 299–307.
29. Liebig C, Ayala G, Wilks J, et al. Perineural invasion is an independent predictor of outcome in colorectal cancer. *J Clin Oncol*. 2009;27: 5131–5137.
30. Wang J, Cai Y, Yu W, Ren C, Spencer DM, Ittmann M. Pleiotropic biological activities of alternatively spliced TMPRSS2/ERG fusion gene transcripts. *Cancer Res*. 2008;68:8516–8524.
31. Martinez-Pineiro L, Dahiya R, Nunes LL, Tanagho EA, Schmidt RA. Pelvic plexus denervation in rats causes morphologic and functional changes of the prostate. *J Urol*. 1993;150:215–218.
32. McVary KT, McKenna KE, Lee C. Prostate innervation. *Prostate Suppl*. 1998;8:2–13.
33. Vaalasti A, Alho AM, Tainio H, Hervonen A. The effect of sympathetic denervation with 6-hydroxydopamine on the ventral prostate of the rat. *Acta Histochem*. 1986;79:49–54.
34. Lujan M, Paez A, Llanes L, Angulo J, Berenguer A. Role of autonomic innervation in rat prostatic structure maintenance: a morphometric analysis. *J Urol*. 1998;160:1919–1923.
35. Lamano-Carvalho TL, Favaretto AL, Petenusci SO, Kempinas WG. Prepubertal development of rat prostate and seminal vesicle following chemical sympathectomy with guanethidine. *Braz J Med Biol Res*. 1993;26:639–646.
36. Lang K, Drell TL, 4th, Lindecke A, et al. Induction of a metastatogenic tumor cell type by neurotransmitters and its pharmacological inhibition by established drugs. *Int J Cancer*. 2004;112:231–238.

37. Shi M, Liu D, Duan H, et al. The beta2-adrenergic receptor and Her2 comprise a positive feedback loop in human breast cancer cells. *Breast Cancer Res Treat*. 2011;125:351–362.

38. Palm D, Lang K, Niggemann B, et al. The norepinephrine-driven metastasis development of PC-3 human prostate cancer cells in BALB/c nude mice is inhibited by beta-blockers. *Int J Cancer*. 2006;118:2744–2749.

39. Murtola TJ, Tammela TL, Maattanen L, Ala-Opas M, Stenman UH, Auvinen A. Prostate cancer incidence among finasteride and alpha-blocker users in the Finnish Prostate Cancer Screening Trial. *Br J Cancer*. 2009;101:843–848.

40. Sahu A, Phelps CP, White JD, Crowley WR, Kalra SP, Kalra PS. Steroidal regulation of hypothalamic neuropeptide Y release and gene expression. *Endocrinology*. 1992;130:3331–3336.

SUPPORTING INFORMATION

Additional Supporting Information may be found online in the supporting information tab for this article.